Official Journal of CIOMP
elight.springeropen.com

RESEARCH ARTICLE

Open Access

Broadband continuous supersymmetric transformation: a new paradigm for transformation optics

Jieun Yim[1], Nitish Chandra[2], Xilin Feng[3], Zihe Gao[1], Shuang Wu[1], Tianwei Wu[1], Haoqi Zhao[3], Natalia M. Litchinitser[2*] and Liang Feng[1,3*]

Abstract

Transformation optics has formulated a versatile framework to mold the flow of light and tailor its spatial characteristics at will. Despite its huge success in bringing scientific fiction (such as invisibility cloaking) into reality, the coordinate transformation often yields extreme material parameters unfeasible even with metamaterials. Here, we demonstrate a new transformation paradigm based upon the invariance of the eigenspectra of the Hamiltonian of a physical system, enabled by supersymmetry. By creating a gradient-index metamaterial to control the local index variation in a family of isospectral optical potentials, we demonstrate broadband continuous supersymmetric transformation in optics, on a silicon chip, to simultaneously transform the transverse spatial characteristics of multiple optical states for arbitrary steering and switching of light flows. Through a novel synergy of symmetry physics and metamaterials, our work provides an adaptable strategy to conveniently tame the flow of light with full exploitation of its spatial degree of freedom.

Keywords: Supersymmetry, Transformation optics, Metamaterials, Integrated photonics

1 Introduction

Our attempts at bending light on demand and arbitrarily transforming its spatial characteristics are rooted in the fundamentals of electromagnetics. The form-invariance of Maxwell's equations under coordinate transformations led to the formulation of transformation optics [1, 2]—the correspondence between the coordinate system and material parameters. Their equivalence allows electromagnetic field in a given coordinate system to be rearranged by designing the medium with the corresponding, spatially dependent dielectric permittivity and magnetic permeability, having consequently opened avenues to a series of intriguing functionality such as invisibility cloaking [3–8], illusion optics [9], etc. Nevertheless, although the excellent design flexibility provided by metamaterials [10–17] enables a wide range of inhomogeneous and anisotropic optical properties, experimental realization of transformation optics, especially in the optical regime, has been in a stalemate for a decade because of optical extremity and singularity often resulting from the transformation. Additionally, in the original resonant meta-atom-based implementation, transformation optics is confined to narrowband operation [4, 5]. Therefore, new schemes towards transformation optics with broadband parameter values within their achievable limits have become necessary. For example, conformal mapping [18, 19] with spatially varying the local index of refraction has been demonstrated to perform the coordinate transformation using inhomogeneous Si nanostructures [20, 21], yielding delicate phase-front control for multicolor carpet cloaking. This approach elucidated the possibility of the exploitation of gradient-index (GRIN) [22, 23] to warp the space, but to

*Correspondence: natalia.litchinitser@duke.edu; fenglia@seas.upenn.edu

[1] Department of Materials Science and Engineering, University of Pennsylvania, Philadelphia, PA 19104, USA
[2] Department of Electrical and Computer Engineering, Duke University, Durham, NC 27708, USA
Full list of author information is available at the end of the article

achieve richer functionality other than bending the trajectories, a paradigmatic shift beyond traditional coordinate transformation is further required.

Another intrinsic principle to formulate the transformation of a physical system is observing its Hamiltonian under transformation. For example, the invariance of the Hamiltonian under symmetry operation [24–26] endows us with insights into how a system can be transformed with a conserved quantity. In particular, supersymmetry (SUSY) [27], which originated from the description of the transformation between bosons and fermions [28], features the degenerate eigenenergy spectra between two distinct Hamiltonians, which has facilitated advanced control of the spatial characteristics of light [29–31]. For example, designed by unbroken SUSY under which the unpaired ground state exists between the original and the superpartner Hamiltonians, strategic coupling between the original optical system and its dissipative superpartner has triggered intriguing applications such as high-radiance single-mode microlaser arrays [32, 33] and mode division multiplexing [34]. These previous experimental studies are based on lattice Hamiltonians, which can be factorized via matrix operation, and hence they constructed systems composed of a number of coupled discrete elements corresponding to coupled waveguides or resonators. In contrast, the extended method of SUSY that can generate an infinite number of strictly isospectral potentials has remained experimentally unexplored, since it requires an intrinsically different approach to realize arbitrary potentials, while its mathematical framework turns out to be ideal for the continuous Hamiltonian transformation to enable a distinct scenario for transformation optics [35, 36] other than the traditional coordinate transformation. Here, we report the first experimental demonstration of continuous SUSY transformation by designing a novel GRIN metamaterial on a Si platform. We utilize the synergy of supersymmetry and the metamaterial to design spatially varying dielectric permittivity, which constitutes a two-dimensional map where arbitrary transformations are prescribed simultaneously to multiple optical states for routing, switching, and spatial mode shaping, while strictly maintaining their original propagation constants. Our result features broadband continuous SUSY transformation in optics, illuminating a novel path to fully utilizing the spatial degrees of freedom on a chip for versatile photonic functionalities.

2 Results and discussion

Owing to the mathematical correspondence between the Schrödinger equation and the Helmholtz equation, we formulate the SUSY transformation by describing the potential of the Hamiltonian using the inhomogeneously distributed refractive index $n(x)$ in the transverse dimension of an optical system. Likewise, the eigenvalue spectrum of the Hamiltonian is represented by the spectrum of the propagation constants calculated from $n(x)$ (See Methods). For an original optical potential $n_0(x)$, SUSY transformation [28, 37, 38] leads to a family of isospectral optical potentials $n_f(x)$ with a free parameter α_i:

$$n_f^2(x;\alpha_i) = n_0^2(x) + \frac{2}{k_0^2}\frac{d}{dx}\left(\frac{1}{I_m(x)}\frac{dI_m(x)}{dx}\right) \tag{1}$$

where $I_m(x) = \int_{-\infty}^{x} \psi_m^2\left(x'\right)dx' + \alpha_i$, and $\psi_m(x)$ is the m^{th} eigenstate of $n_0(x)$. By this means, one can conveniently delete the eigenstate ψ_m and reinstate a new ψ_m with the same propagation constant but different spatial characteristics of light depending on parameter α_i. Hence, this mathematical operation can be understood as a reshaping process of $n_0(x)$, enabling the isospectral transformation of light by continuously varying the parameter α_i (and thus $n_f(x;\alpha_i)$) in the z direction (Fig. 1a). Since the choice of ψ_m is associated with α_i, Eq. 1 can be iterated n times with different ψ_m and α_i to generate a n-parameter (i.e., $\{\alpha_1, \alpha_2, \ldots, \alpha_n\}$) family of isospectral potentials, which offers sufficient design flexibility appropriate for transformation optics. Note that for a normalizable ψ_m, $n_f(x;\alpha_i)$ is guaranteed to be non-singular as long as $\alpha_i < -1$ or $\alpha_i > 0$.

Here, based on a Si waveguide system where the eigenstates bound in the transverse plane propagate along the z direction, we design a full 2D map of spatially dependent refractive index $n(x,z)$ (Fig. 1a) in which the trajectories and the transverse mode profiles of three guided eigenstates are controlled, by substituting $n_0^2(x) = a + be^{-\left(\frac{x-d}{c\lambda}\right)^2}$ with $a = 2.31, b = 1.4, c = 0.8$, and $d = 6.1875\mu m$, and the wavelength of light $\lambda =$ 1550 nm into Eq. 1. Since we consider three eigenstates well guided in the given $n_0(x)$, SUSY transformation is applied to $n_0(x)$ at each z coordinate twice: the first with ψ_m and parameter α_1, and the second with ψ_n and α_2, where m and n denote the order numbers of the selected eigenstates (See Methods). After such two-parameter transformation, $n_0(x)$ is transformed to $n_f(x)$ with respect to ψ_m and ψ_n as well as α_1 and α_2. In practice, the index distribution at $z = 0.5L$ is set to be $n_0(x)$ (i.e., $n_f(x) \to n_0(x)$ as $|\alpha_i| \to \infty$), where all three eigenstates are guided at the center. From $z = 0.5L$ towards either $z = 0$ or $z = L$, $|\alpha_i|$ reduces, and $n_f(x)$ consequently features high-index regions newly emerging at both sides of the remaining high-index region in the center, such that two optical states are separately guided away from the center (Fig. 1b). In this scenario, a series of $n_f(x)$ with continuously changing $\alpha_1(z)$ and $\alpha_2(z)$ are

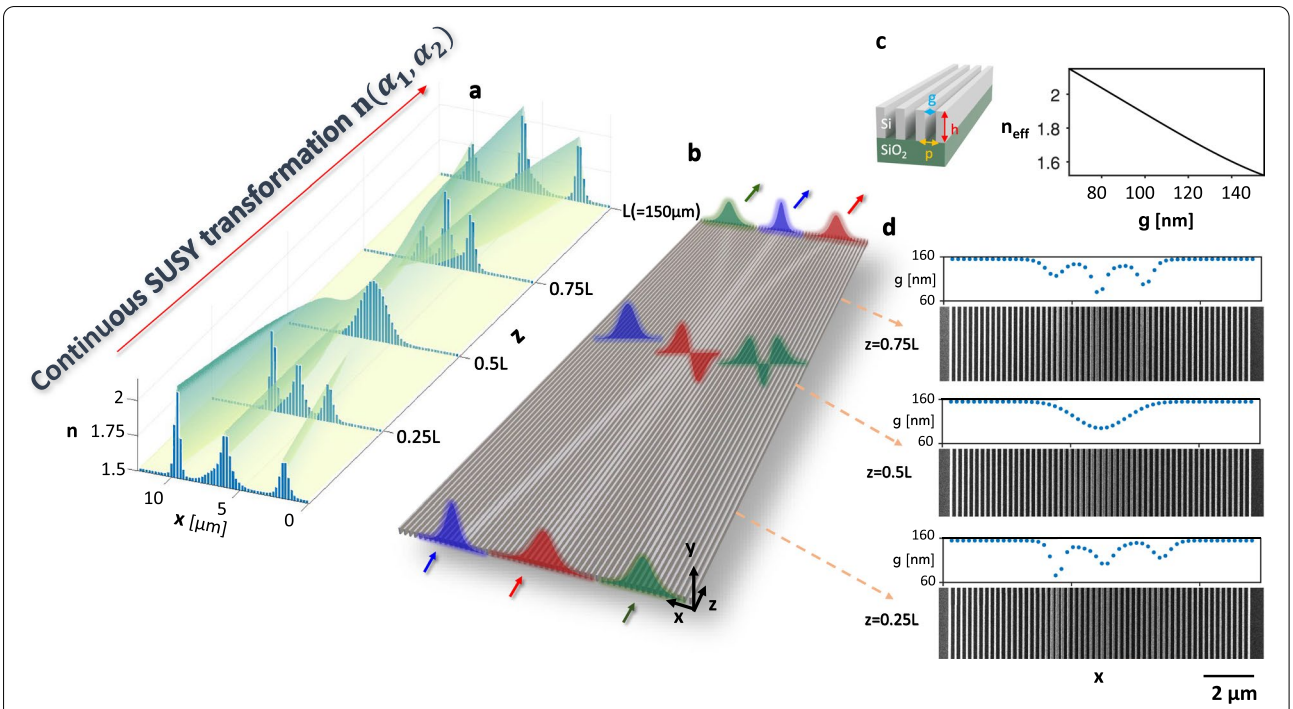

Fig. 1 Continuous SUSY transformation optics and its demonstration on a Si chip. **a** Two-dimensional refractive index distribution $n(x,z)$ designed by SUSY transformation with continuously varying parameter α_i in Eq. 1. $n(x)$ is shown at five different z coordinates: $z = 0, 0.25L, 0.5L, 0.75L$, and L, where $L = 150$ μm, where the index profile is discretized in the x direction for the design implementation. **b** GRIN metamaterial designed to substantiate $n(x,z)$, where different optical states (blue, red, green) with different propagation constants can propagate with spatial characteristics and directions dictated by the SUSY transformation. **c** Schematic of the on-chip subwavelength Si metamaterial for local index tuning, with physical parameters: $h = 300$ nm and $p = 225$ nm, and its numerically simulated relationship between the effective refractive index (n_{eff}) and the size of the air gap (g) at the wavelength of 1550 nm (Supplementary Additional file 1: Fig. S2). **d** Scanning electron microscope images of the fabricated Si GRIN metamaterial and its prescribed gap distribution at three different z coordinates: $z = 0.25L, 0.5L$, and $0.75L$, corresponding to $n(x,z)$ in **a**

connected along the propagation direction z to form the 2D map of $n(x,z)$ (Additional file 1: Fig. S1). If the transformation of $\alpha_i(z)$ is adiabatic, the guided eigenstates can propagate through the variations of $n_f(x;\alpha_i)$ in a lossless manner because of their identical spectra of propagation constants guaranteed by SUSY. Therefore, by tagging an optical state with its propagation constant, the continuous SUSY transformation facilitates arbitrary routing and switching of the optical state, even allowing it to cross the lightpaths of other states without any perturbation to their original properties regardless of the number of optical states intersecting one another.

In order to realize the spatially inhomogeneous index map of $n(x,z)$, we devise a GRIN metamaterial made of deep subwavelength Si nanostructures with a period of 225 nm in the x direction (Figs. 1a and b). The transverse index profile $n(x)$ is discretized with the same period into the local indices, and the corresponding GRIN metamaterial is tailored by adjusting the filling ratio of Si (i.e., the size of the air gap g) that is related to the local effective index n_{eff} for the fixed height h and period p (Fig. 1c). Note that $n(x,z)$ in the design implementation represents the local $n_{eff}(x)$ of quasi-TM modes of the Si GRIN metamaterial in the xy plane at a given z, and nonetheless, the SUSY transformation remains valid by replacing $n(x)$ with $n_{eff}(x)$ (See Methods). With optimized physical parameters to satisfy the required maximum index contrast (i.e., $n_{max} - n_{min}$), the metamaterial that features air gaps locally tailored in the xz plane to emulate a GRIN medium undergoing the continuous SUSY transformation is fabricated on a Si-on-insulator platform with a cladding layer of air (Fig. 1d and See Methods). In this case, three distinct quasi-TM modes are guided in the on-chip GRIN metamaterial, subject to the continuous SUSY transformation during the propagation. Although exact isospectral transformation only occurs at the wavelength of 1550 nm, approximately the same performance of the SUSY transformation optics is anticipated in the broad range of input wavelengths, as estimated by calculating the effective mode indices at different wavelengths for the refractive index potential transformed for the wavelength of 1550 nm (Additional file 1: Fig. S3). In the wavelength range of interest from 1460 to 1570 nm, less than 0.6% variation of the modal indices is expected

between $z = 0$ and $z = 0.5L$ in our design of $n(x, z)$. Such a quasi-flat dispersion originates from the small variation of the potentials after the SUSY transformation when the wavelength used for the transformation is varied within the range of 110 nm. Intrinsic material dispersion and waveguide dispersion can be effectively minimized with the right material choice and optimized physical parameters of the metamaterial.

The virtue of SUSY transformation in optics is the controllability of light with increased spatial degrees of freedom in association with the eigenstates (i.e., optical modes), which allows them to be arbitrarily routed, switched, and spatially evolve while preserving their propagation constants secured by SUSY. In this regard, a complicated spatial distribution of light linked to a specific eigenstate, which is difficult in reality to excite directly by using an external light source, can be achieved by first exciting an eigenstate with a fundamental-mode profile and transforming its spatial profile in a metamaterial designed by SUSY transformation. For example, all the eigenstates displayed at $z = 0$ (Figs. 2a and c) are fundamental modes, but they are transformed along the z direction to possess the spatial characteristics of the high-order modes at $z = 0.5L$, while their propagation constants remain identical to those of the corresponding fundamental modes at $z = 0$, respectively. At $z = L$, the eigenstates revert back to fundamental modes, but they are directed toward different x coordinates, indicating that their trajectories can also be arbitrarily maneuvered. Such continuous transformation is validated by numerical simulations in which light propagates through the GRIN medium, realized by varying the gap distribution along the z direction (Figs. 2b and d). The simulated intensity map explicitly reveals that the SUSY transformation is a powerful toolbox to conveniently steer the light and transform its transverse spatial profile. One thing to note is that depending on the $n(x)|_{z=0.5L}$, more complex spatial characteristics of light are attainable in this manner. Additionally, the asymmetric (Figs. 2a and b) and symmetric (Figs. 2c and d) designs exemplify the versatile reconfigurability of the SUSY transformation, enabling spatial switching of the different optical states while keeping individual propagation constants intact by SUSY. Therefore, even though two designs differ in the region from $z = 0.5L$ to $z = L$ since different combinations of ψ_m and ψ_n are applied in two SUSY transformations, the

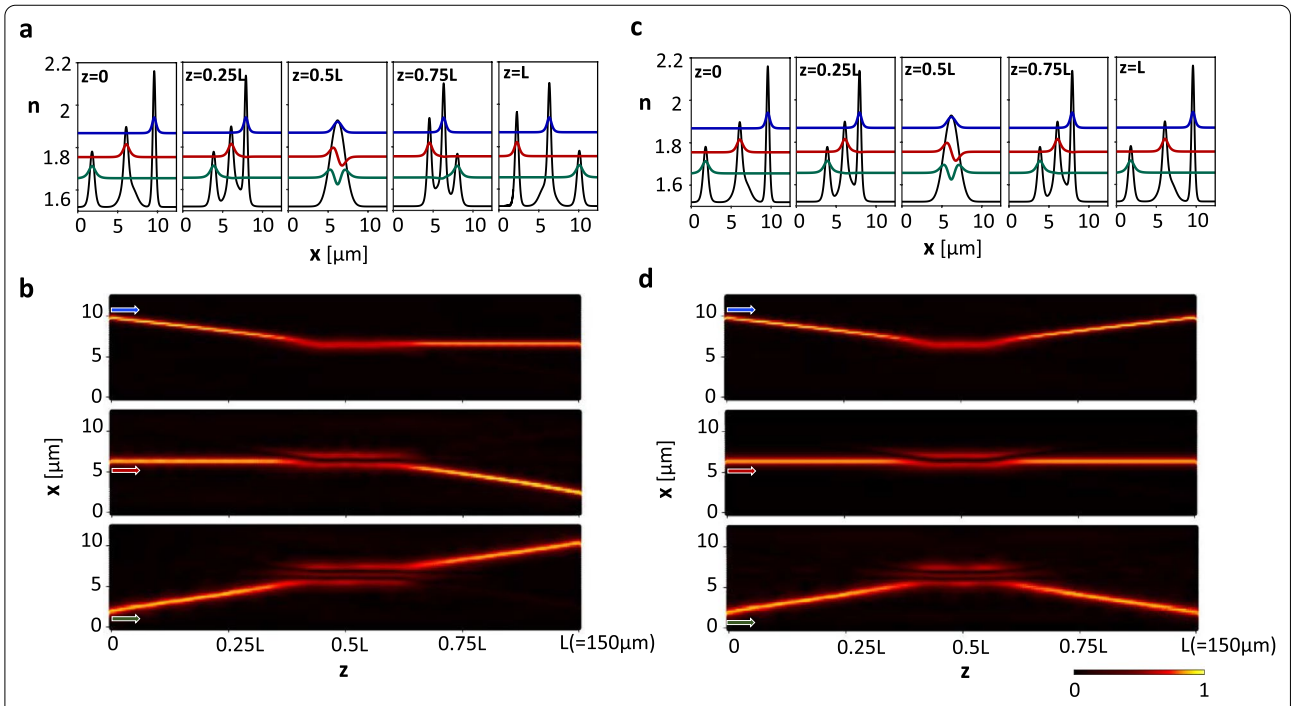

Fig. 2 Numerical simulation for asymmetric and symmetric configurations of SUSY transformation optics. **a**, **c** The optical potentials and the corresponding mode profiles of three eigenstates (blue, red, green) at five different z coordinates at $z = 0, 0.25L, 0.5L, 0.75L$, and L, for asymmetric **a** and symmetric **c** designs. The offsets of the mode profiles indicate their effective mode indices from high, middle to low: $n_{blue} = 1.868$, $n_{red} = 1.755$, and $n_{green} = 1.656$. **b**, **d** Simulated electric field intensity in the GRIN metamaterials with prescribed gap distributions for asymmetric **b** and symmetric **d** designs. From the top, center, to bottom, different optical states are excited at $z = 0$, as denoted by the colors of the arrows, corresponding to the blue, red, and green eigenstates, respectively, in **a** and **c**. It is evident that fundamental mode excitations from different input ports transform to the fundamental, first-order, and second-order modes from $z = 0$ to $z = 0.5L$, consistent with the design in **a** and **c**

invariance of the eigenspectra of the Hamiltonian always holds: the effective indices of the three different eigenstates, which are denoted by the offset of each eigenstate (Figs. 2a and c), remain the same throughout the entire z dimension. Furthermore, since our system is a linear system, and the eigenstates are orthogonal, if all of three states are excited at $z = 0$, each of them will be separately and simultaneously steered to its designated x coordinate at $z = L$ to respect the isospectrality.

Broadband light steering and spatial switching through SUSY transformations were experimentally validated by characterizing the normalized transmission spectra of the two Si GRIN metamaterials corresponding to the asymmetric and symmetric designs illustrated in Fig. 2, respectively. The transmission spectra were measured at three outputs at $z = L$ (O1, O2, O3) for three different inputs at $z = 0$ (I1, I2, I3) using a tunable laser with a wavelength range from 1460 to 1570 nm (Figs. 3a and c). In experiments, three single-mode waveguides were connected to the GRIN metamaterial at $z = 0$ to launch the fundamental mode excitations from the inputs; similarly, three single-mode waveguides were also attached at $z = L$ to direct the output signals for detection. The propagation constants of the connected single-mode waveguides were designed to closely match those of the three eigenstates steered in the GRIN metamaterial, thereby minimizing mode mismatch and maximizing the coupling efficiencies. As a result, the characterized spectra present near-unity broadband transmission from inputs to their corresponding outputs over the wavelength range of 110 nm, in both asymmetric and symmetric designs. Specifically, the transmission matrix can be retrieved, where each element M_{ji} denotes normalized transmitted power from input i to output j (Figs. 3b and d), showing high transmission of 0.94 on average with negligible crosstalk between neighboring channels at the wavelength of 1550 nm in both asymmetric and symmetric designs.

Broadband transformation of spatial characteristics of light enabled by the SUSY transformation was verified by imaging the intensity profile of guided light at the midpoint along z of the GRIN metamaterial ($z = 0.5L$) over the entire range of the tunable laser (Fig. 4a). Light coupled into the metamaterial as a fundamental mode with a specific propagation constant is spatially transformed to the optical state with an identical propagation constant but a different field profile. In this scenario, excitations at three different input ports take different transformation routes, such that their spatial characteristics evolve differently (Figs. 4b–d) while their propagation constants remain unchanged during the evolution by SUSY. All three spatial modes are the eigenstates of the GRIN metamaterial at $z = 0.5L$, so they are simultaneously supported without crosstalk because of their inherent orthogonality. The clear nodes observed in the images agree well with the calculated modal field profiles at $z = 0.5L$ as shown in Fig. 2, definitively confirming the efficacy of isospectral SUSY transformation despite inevitable perturbation caused by imperfect fabrication leading to the asymmetry of the mode profile. Moreover, the far-field diffraction patterns of optical states reassure that the lobes present in each state contain the same relative phase information as theoretically predicted (Additional file 1: Fig. S5).

3 Conclusion

Our work opens up possibilities of bringing the symmetry of Hamiltonian into the realm of optics by constructing a metamaterial that can emulate arbitrary potentials to achieve an advanced control of light through transforming the optical media. Especially, the interplay of supersymmetry and a metamaterial demonstrated in this study can contribute to the increase of the spatial degree of freedom in integrated photonics by facilitating arbitrary light steering, switching, and sophisticated spatial mode shaping of light without introducing any perturbation to the propagation constants of all the eigenstates. Our continuous SUSY transformation approach is scalable to a higher number of eigenstates and free parameters, and also applicable to more complicated index distribution, thereby creating an ideal platform for on-chip space-division multiplexing in information technologies. Additionally, further extending the SUSY transformation into higher dimensions [33] may provide a design strategy to exploit the full potential of metamaterials in the three-dimensional space.

4 Methods

4.1 Isospectral supersymmetric transformation [28, 39]

For a 1D system, the Schrödinger equation can be written as:

$$\left(-\frac{d^2}{dx^2} + V\_(x)\right)\psi_m(x) = E_m\psi_m(x) \tag{2}$$

where ψ_m is the m^{th} eigenfunction with eigenenergy E_m for the given potential $V\_$. The Hamiltonian $H = -\frac{d^2}{dx^2} + V\_(x)$ can be factorized as $H = A^{\dagger}A$, where $A = \frac{d}{dx} + W$ and $A^{\dagger} = -\frac{d}{dx} + W$. Here, W is the superpotential defined as $-\frac{\psi_0'}{\psi_0}$, and ψ_0 is the ground state eigenfunction. Consequently, the original potential (V_-) and the supersymmetric potential (V_+) are

$$V_{\pm} = W^2 \pm W'. \tag{3}$$

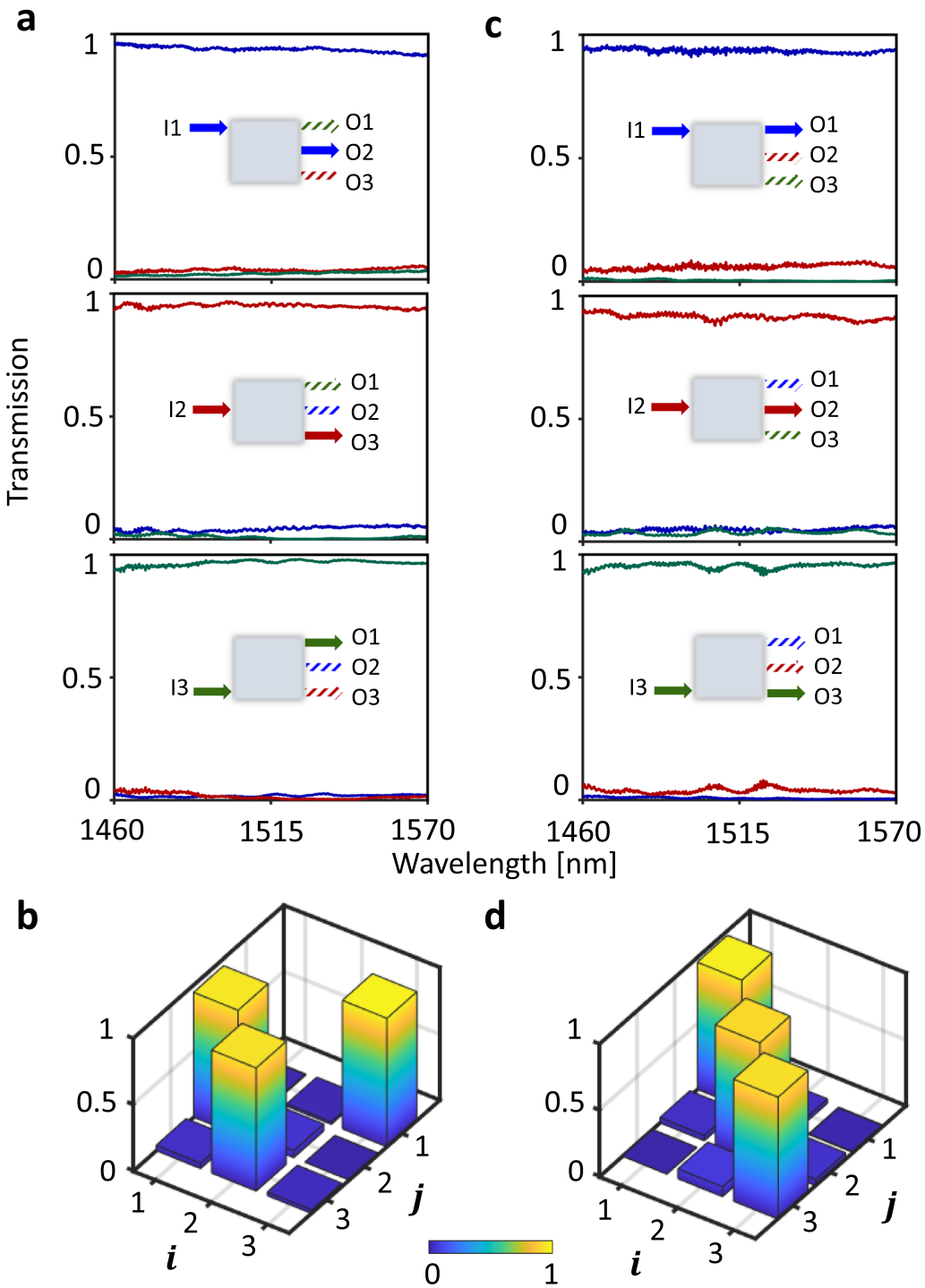

Fig. 3 Experimental characterization of broadband on-chip continuous SUSY transformation. **a**, **c** Normalized transmittance spectra of the asymmetric **a** and symmetric **c** Si GRIN metamaterials. Top, middle, and bottom panels denote three single-mode inputs from top to bottom: I1, I2, and I3, respectively. The transmission spectra are measured at three outputs: O1, O2, and O3. Note that in both asymmetric **a** and symmetric **c** cases, three output intensities are normalized to their sum. The colors of the line plots and the arrows of the insets (blue, red, green) coincide with the colors of the eigenstates in Fig. 2, according to their corresponding optical modes. **b**, **d** Measured transmission (*M*) matrices where M_{ji} stands for power transmission from input *i* to output *j* at the wavelength of 1550 nm, retrieved from **a** and **c**, respectively

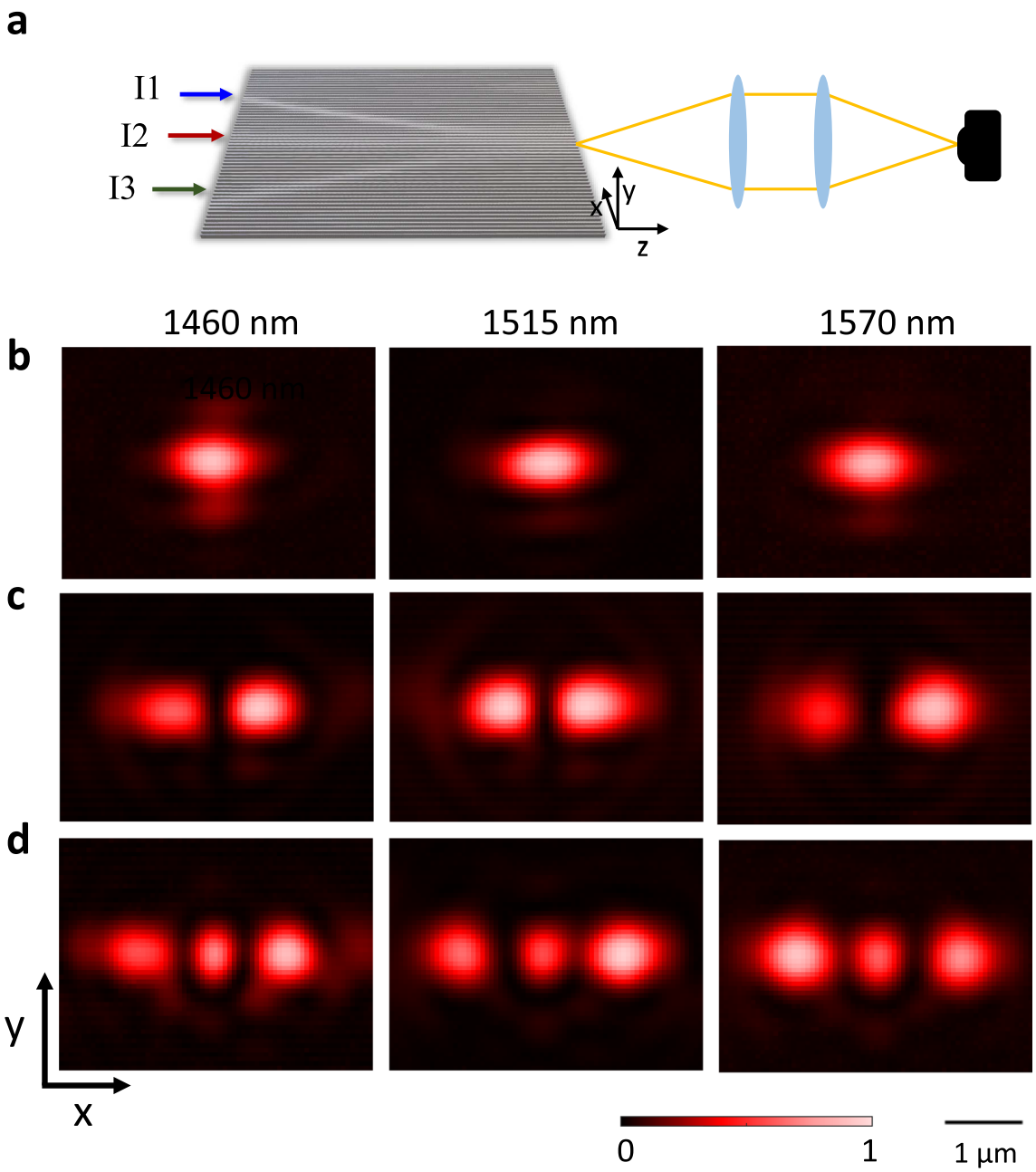

Fig. 4 Experimental characterization of transverse spatial characteristics of light achieved by broadband SUSY transformation. **a** Schematic of the imaging system to characterize the transverse field intensity at the midpoint along z in the GRIN metamaterial (i.e., $z = 0.5L$). A $4f$ imaging is performed for appropriate magnification. **b, c, d** Measured intensity profiles in the xy plane when the light was launched at different inputs from top to bottom: I1, I2, and I3, in a broad wavelength range from 1460 nm (left column), 1515 nm (middle column), to 1570 nm (right column). The results experimentally confirm that fundamental mode excitations from different input ports (I1, I2, and I3) transform to the fundamental, first-order, and second-order modes as they propagate from $z = 0$ to $z = 0.5L$, respectively, consistent with the theoretical design in Fig. 2

This is the case of the first-order unbroken SUSY, under which the original Hamiltonian ($H = A^{\dagger}A$) and the supersymmetric Hamiltonian ($H^{\dagger} = AA^{\dagger}$) share the identical eigenvalue spectra except for the ground state. To extend the SUSY transformation beyond the unbroken case, here we find a generalized form of the superpotential $\widehat{W}$ which satisfies

$$V_{+} = \widehat{W}^{2} + \widehat{W}^{'} = W^{2} + W^{'} \tag{4}$$

We solve this differential equation for $\widehat{W}$ and obtain

$$\widehat{W}(x;\alpha_i) = W(x) + \frac{d}{dx}\ln(I_m(x)) \tag{5}$$

where $I_m(x) = \int_{-\infty}^{x} \psi_m^2\left(x'\right)dx' + \alpha_i$, and α_i is a free parameter that can be continuously varied. Here, by using this generalized superpotential, we define $\widehat{V}_f = \widehat{W}^2 - \widehat{W}'$, and by using Eq. 3, Eq. 4, and Eq. 5, we obtain.

$$\widehat{V}_f = V_- - 2\frac{d}{dx}\left(\frac{1}{I_m(x)}\frac{dI_m(x)}{dx}\right) \tag{6}$$

where $\widehat{V}_f$ represents a family of isospectral potentials and the original potential V_- belongs to the isospectral family for $\alpha_i \to \infty$.

In our work, we apply the effective index method to realize a 1D map of transverse refractive index $n(x)$ by extracting the indices of the quasi-TM mode in 2D geometries in the xy plane. The electric field of the quasi-TM mode propagating along the z direction in a dielectric waveguide is described as $\vec{E} = (\vec{E}_y + \vec{E}_z)e^{ik_z z}$ where the dominant y component can be written with separable variables.

$$\vec{E}_y = \hat{y}\psi(x)\Phi(y;x)e^{ik_z z} \tag{7}$$

Here, $\psi(x)$ and $\Phi(y;x)$ are two different amplitudes associated with the field confinement in the x and y directions, and k_z is real, thus equal to the propagation constant. We assume that $\Phi(y;x)$ is a slowly varying function along x ($\frac{\delta\Phi}{\delta x} \simeq 0$). By solving the Helmholtz equation, we deduce:

$$\frac{d^2\Phi(y;x)}{dy^2} + k_0^2 n^2(x,y)\Phi(y;x) = k_0^2 n_{eff}^2(x)\Phi(y;x) \tag{8}$$

$$\frac{d^2\psi(x)}{dx^2} + k_0^2 n_{eff}^2(x)\psi(x) = k_z^2\psi(x) \tag{9}$$

where $k_0 = \frac{2\pi}{\lambda_0}$ with the free space wavelength of λ_0. Therefore, once we have the distribution of the local effective index $n_{eff}(x)$ from Eq. 8, we can solve Eq. 9 to obtain the mode index $n_{mode} = \frac{k_z}{k_0}$ of the entire 2D geometry.

More importantly, the comparison between Eq. 2 and Eq. 9 evidently exhibits the mathematical correspondence: $V_-(x)$ in quantum mechanics can be described by $k_0^2 n_{eff}^2(x)$, and eigenenergy E_m can be replaced by k_z^2. Therefore, we can bring the mathematical framework of SUSY into the realm of optics, which leads to Eq. 1 in the main text. From there, we can calculate numerous potentials of $n_{eff}^2(x)$ that yield the same eigenvalue spectra of k_z^2, with respect to the continuously varying free parameter α_i.

4.2 Generation of refractive index distribution by SUSY transformation

The free parameter α_i is an integral constant, which arises when the generalized superpotential $\widehat{W}$ is obtained from the differential equation Eq. 4. As a result, a different value of α_i generates a different superpotential $\widehat{W}$, which eventually leads to a different optical potential, while the isospectrality still remains, following the mathematical framework of supersymmetry. In this regard, owing to the mathematical relation between $n_f(x;\alpha_i)$ and α_i in Eq. 1, $n_f(x;\alpha_i)$ is nearly the same as $n_0(x)$ when $|\alpha_i|$ is large. In contrast, as the value of α_i approaches from -∞ to -1 or from ∞ to 0, $n_f(x;\alpha_i)$ becomes more distinguishable from $n_0(x)$. This transformation occurs such that the selected eigenstate $\psi_m(x)$ for the transformation moves away farther from the original potential. At the limit of $\alpha_i \to -1^-$ or $\alpha_i \to 0^+$, singularity of the potential and $\psi_m(x)$ after the transformation occurs at an infinite value of x (i.e. x = -∞ or ∞), and hence $\psi_m(x)$ is no longer square integrable. In this case, the transformation forces the bound state $\psi_m(x)$ to vanish from the $n_0(x)$ while the other bound states remain bound respecting the isospectrality [40]. Therefore, the values of α_1 and α_2 in our study dictate the degree of transformation of $n_0(x)$ in relation to two eigenstates ψ_m and ψ_n with the condition of $\alpha_i < -1$ or $\alpha_i > 0$ to avoid any singularity in $n(x)$. In our design process for the index distribution, SUSY transformation is applied at each z coordinate to the original index distribution $n_0(x)$ (as defined in the main text) twice by substituting into Eq. 1 the values of α_1 and α_2, respectively, which are continuously varied along the z direction (Additional file 1: Fig. S1a and S1b). α_1 and α_2 should be individually controlled to ensure the adiabatic change of the refractive index distribution $n(x)$ along the z direction. At $z = 0.5L$, $n(x)$ is close to $n_0(x)$ owing to the large values of $|\alpha_1|$ and $|\alpha_2|$. From $z = 0.5L$ to $z = 0$, $|\alpha_1|$ and $|\alpha_2|$ are gradually reduced to adiabatically change $n(x)$ in association with ψ_3 and ψ_1, respectively. Here, α_1 is decreased to near 0 and α_2 is increased to near -1, and the signs of α_1 and α_2 are opposite because their signs are related to the $+x$ or $-x$ direction of the spatial change of $n(x)$. Similarly, from $z = 0.5L$ to $z = L$, α_1 is decreased to near 0 and α_2 is increased to near -1 with ψ_2 and ψ_3 being used in the transformation, and their variations are different from those in the region of $z = 0$ to $0.5L$ because of different choices of the eigenstates. The resulting asymmetric

$n(x,z)$ (Additional file 1: Fig. S1c) features a smooth transformation of the refractive index along the z direction, in which three eigenstates are accordingly altered during the propagation with unchanged mode indices, as presented in the asymmetric design illustrated in Fig. 2 and Fig. 3 of the main text.

4.3 Sample fabrication

The sample was fabricated by electron beam lithography and reactive ion etching (Additional file 1: Fig. S4). The first step was to spin-coat the Si-on-insulator wafer by 6% Hydrogen Silsesquioxane (HSQ) negative resist, which was a 2:3 mixture of FOX15 and Methyl isobutyl ketone (MIBK). After electron beam patterning, the resist was developed by immersing into the MF CD-26 at 60 °C for 40 s and then rinsing in DI water for 30 s. The resist in the exposed areas remained on the sample and acted as a hard mask for reactive ion etching. Subsequently, the Si layer was etched via reactive ion etching in SF_6/C_4F_8 plasma. Finally, the sample was cleaved after coating a protection layer of PMMA to make a sharp facet for the output waveguides and the PMMA layer was fully removed after cleaving. The Si GRIN metamaterial used for the characterization of the transverse mode profile at $z = 0.5L$ (as shown in Fig. 4) shares the same design as Fig. 1b from $z = 0$ up to $z = 0.5L$ but has an extended region beyond $z = 0.5L$, where the gap distribution no longer changes along the z direction. This strategy guarantees that we can observe the light intensity profile effectively at $z = 0.5L$ after cleaving the chip at $z > 0.5L$.

Supplementary Information

The online version contains supplementary material available at https://doi.org/10.1186/s43593-022-00023-1.

Additional file 1: Figure S1. Generation of refractive index distribution by SUSY transformation with a free parameter α_j. **Figure S2.** Simulation results for the effective index of the Si metamaterial. **Figure S3.** The dispersion of the mode indices of the eigenstates calculated by SUSY transformation in a broad range of operation wavelengths from 1460 nm to 1570 nm. **Figure S4.** Fabrication and SEM images of the sample. **Figure S5.** Far-field diffraction pattern of the optical states achieved by SUSY transformation.

Acknowledgements
This work was partially supported by NSF through the University of Pennsylvania Materials Research Science and Engineering Center (MRSEC) (DMR-1720530) and carried out in part at the Singh Center for Nanotechnology, which is supported by the NSF National Nanotechnology Coordinated Infrastructure Program under grant NNCI-1542153.

Author contributions
JY, NC, NML, and LF designed the experiment. JY and NC performed the theory of SUSY. JY conducted the design and performed the numerical simulation. XF fabricated the samples. JY, ZG, SW, TW, and HZ performed the measurements. LF and NML supervised the project. All authors contributed to data analysis and manuscript preparation.

Funding
U.S. Army Research Office (ARO) (W911NF-19–1-0249 and W911NF-18–1-0348); National Science Foundation (NSF) (CMMI-2037097).

Availability of data and materials
Supporting data and materials are given in the supplementary information. Additional data are available from the corresponding author upon reasonable request.

Declarations

Competing interests
The authors declare no competing interests.

Author details
[1]Department of Materials Science and Engineering, University of Pennsylvania, Philadelphia, PA 19104, USA. [2]Department of Electrical and Computer Engineering, Duke University, Durham, NC 27708, USA. [3]Department of Electrical and Systems Engineering, University of Pennsylvania, Philadelphia, PA 19104, USA.

Received: 22 July 2022 Revised: 8 August 2022 Accepted: 10 August 2022
Published online: 12 September 2022

References

1. U. Leonhardt, Science **312**, 1777 (2006)
2. J.B. Pendry, D. Schurig, D.R. Smith, Science **312**, 1780 (2006)
3. A. Alù, N. Engheta, Phys. Rev. E **72**, 016623 (2005)
4. D. Schurig, J.J. Mock, B.J. Justice, S.A. Cummer, J.B. Pendry, A.F. Starr, D.R. Smith, Science **314**, 977 (2006)
5. W. Cai, U.K. Chettiar, A.V. Kildishev, V.M. Shalaev, Nat. Photonics **1**, 224 (2007)
6. I.I. Smolyaninov, V.N. Smolyaninova, A.V. Kildishev, V.M. Shalaev, Phys Rev Lett **102**, 213901 (2009)
7. T. Ergin, N. Stenger, P. Brenner, J.B. Pendry, M. Wegener, Science **328**, 337 (2010)
8. T. Han, X. Bai, D. Gao, J.T.L. Thong, B. Li, C.-W. Qiu, Phys Rev Lett **112**, 054302 (2014)
9. Y. Lai, J. Ng, H. Chen, D. Han, J. Xiao, Z.-Q. Zhang, C.T. Chan, Phys Rev Lett **102**, 253902 (2009)
10. V.G. Veselago, Sov Phys Usp **10**, 509 (1968)
11. D.R. Smith, W.J. Padilla, D.C. Vier, S.C. Nemat-Nasser, S. Schultz, Phys Rev Lett **84**, 4184 (2000)
12. R.A. Shelby, D.R. Smith, S. Schultz, Science **292**, 77 (2001)
13. A.J. Hoffman, L. Alekseyev, S.S. Howard, K.J. Franz, D. Wasserman, V.A. Podolskiy, E.E. Narimanov, D.L. Sivco, C. Gmachl, Nat Mater **6**, 946 (2007)
14. J. Valentine, S. Zhang, T. Zentgraf, E. Ulin-Avila, D.A. Genov, G. Bartal, X. Zhang, Nature **455**, 376 (2008)
15. J.K. Gansel, M. Thiel, M.S. Rill, M. Decker, K. Bade, V. Saile, G. von Freymann, S. Linden, M. Wegener, Science **325**, 1513 (2009)
16. W. Cai, V.M. Shalaev, *Optical metamaterials: fundamentals and applications* (Springer, New York, 2010)
17. N.I. Zheludev, Y.S. Kivshar, Nat Mater **11**, 917 (2012)
18. J. Li, J.B. Pendry, Phys Rev Lett **101**, 203901 (2008)
19. R. Liu, C. Ji, J.J. Mock, J.Y. Chin, T.J. Cui, D.R. Smith, Science **323**, 366 (2009)
20. J. Valentine, J. Li, T. Zentgraf, G. Bartal, X. Zhang, Nat Mater **8**, 568 (2009)
21. L.H. Gabrielli, J. Cardenas, C.B. Poitras, M. Lipson, Nat Photonics **3**, 461 (2009)
22. D.R. Smith, J.J. Mock, A.F. Starr, D. Schurig, Phys Rev E **71**, 036609 (2005)
23. W.X. Jiang, S. Ge, T. Han, S. Zhang, M.Q. Mehmood, C. Qiu, T.J. Cui, Adv Sci **3**, 1600022 (2016)
24. A. Kodigala, T. Lepetit, Q. Gu, B. Bahari, Y. Fainman, B. Kanté, Nature **541**, 196 (2017)
25. A.B. Khanikaev, G. Shvets, Nat Photonics **11**, 763 (2017)
26. L. Feng, R. El-Ganainy, L. Ge, Nat Photonics **11**, 752 (2017)
27. E. Witten, Nucl Phys B **188**, 513 (1981)

28. F. Cooper, A. Khare, U.P. Sukhatme, *Supersymmetry in quantum mechanics* (World Scientific, River Edge, 2001)
29. M.-A. Miri, M. Heinrich, R. El-Ganainy, D.N. Christodoulides, Phys Rev Lett **110**, 233902 (2013)
30. S. Longhi, Opt Lett **40**, 463 (2015)
31. S. Yu, X. Piao, J. Hong, N. Park, Nat Commun **6**, 8269 (2015)
32. M.P. Hokmabadi, N.S. Nye, R. El-Ganainy, D.N. Christodoulides, M. Khajavikhan, Science **363**, 623 (2019)
33. X. Qiao, B. Midya, Z. Gao, Z. Zhang, H. Zhao, T. Wu, J. Yim, R. Agarwal, N.M. Litchinitser, L. Feng, Science **372**, 403 (2021)
34. M. Heinrich, M.-A. Miri, S. Stützer, R. El-Ganainy, S. Nolte, A. Szameit, D.N. Christodoulides, Nat Commun **5**, 3698 (2014)
35. M.-A. Miri, M. Heinrich, D.N. Christodoulides, Optica **1**, 89 (2014)
36. W. Walasik, N. Chandra, B. Midya, L. Feng, N.M. Litchinitser, Opt Express **27**, 22429 (2019)
37. J. Pappademos, U. Sukhatme, A. Pagnamenta, Phys Rev A **48**, 3525 (1993)
38. D.J.C. Fernández, E. Salinas-Hernández, J Phys A Math Gen **36**, 2537 (2003)
39. T. Tamir, R.C. Alferness, *Guided-wave optoelectronics* (Springer, Berlin, 1990)
40. A. Khare, U. Sukhatme, J Phys A Math Gen **22**, 2847 (1989)